Report of Project MICHIGAN

MECHANICS OF ROTATING PLATES AND PRISMS

W. L. BROWN
C. T. YANG

February 1961

e r

\\ \\ R C ⁷

NOTICES

PREFACE

Project MICHIGAN is a continuing research and development program for advancing the Army's long-range combat-surveillance and target-acquisition capabilities. The program is carried out by a full-time Institute of Science and Technology staff of specialists in the fields of physics, engineering, mathematics, and psychology, by members of the teaching faculty, by graduate students, and by other research groups and laboratories of The University of Michigan.

The emphasis of the Project is upon basic and applied research in radar, infrared, information processing and display, navigation and guidance for aerial platforms, and systems concepts. Particular attention is given to all-weather, long-range, high-resolution sensory and location techniques, and to evaluations of systems and equipments both through simulation and by means of laboratory and field tests.

Project MICHIGAN was established at The University of Michigan in 1953. It is sponsored by the U. S. Army Combat Surveillance Agency of the U. S. Army Signal Corps. The Project constitutes a major portion of the diversified program of research conducted by the Institute of Science and Technology in order to make available to government and industry the resources of The University of Michigan and to broaden the educational opportunities for students in the scientific and engineering disciplines.

Progress and results described in reports are continually reassessed by Project MICHIGAN. Comments and suggestions from readers are invited.

Robert L. Hess
Technical Director
Project MICHIGAN

CONTENTS

FIGURES

TABLE

MECHANICS OF ROTATING PLATES AND PRISMS

ABSTRACT

This is the report of an analysis of rotating plates and prisms from a theoretical viewpoint for the purpose of setting limits on the size and rotational speed of such bodies for scanner applications. The analysis was carried completely through for a fused-quartz elliptical plate rotating about an axis, in the plane which contains a normal to the plate and the major axis, at a 45° angle to the major axis, and for a fused-quartz prism of triangular cross section rotating about an axis through its centroid, normal to the cross section. The analysis indicated that the stresses and displacements are quite large for a 0.5-inch-thick plate with a 9-inch major axis and a $9/\sqrt{2}$-inch minor axis, but negligible for a 6-inch prism whose cross section is an equilateral triangle of 3-inch altitude. The foregoing applies for rotational frequencies of approximately 100 cps, which is a typical operating speed for an infrared scanner.

1
INTRODUCTION

Modern scanning techniques (infrared and other) require the use of mirrors which rotate at extremely high velocities. The high-resolution requirements of the optical systems used for such applications cause some concern about the effects of forces upon the shapes of the mirror surfaces during the process of rotation.

The problems which are the subject of this report lend themselves well to solution by stress functions, which satisfy the equations for equilibrium of the body, continuity of deflection, and certain applicable boundary conditions. The solutions may be used in numerous situations where one is concerned with the mechanics of rotating plates or prisms.

The specific purpose of this report is to give the deflections and stresses for two particular scanning mirrors. However, every attempt has been made to make the solutions general and of a form convenient for application to other situations.

2
SUMMARY OF RESULTS

2.1. DEFLECTIONS AND STRESSES IN ROTATING PLATES

Several problems were solved in an attempt to obtain a comparison of rotating plates of similar shapes. Circular and elliptical plates were of conern in this case, and hence are those used in the calculations.

2.1.1. ROTATING ELLIPTICAL PLATES. The plate to be considered as a numerical example for this analysis is elliptical in shape (Figure 1). It is 0.5 inch thick and has a major axis of 9 inches and a minor axis of $9/\sqrt{2}$ inches. The center of rotation is the center of the ellipse, and the axis rotation makes an angle of 45° with the major axis and 90° with the minor axis. The speed of rotation is assumed to be 5000 rpm. The plate is constructed of fused quartz, although only the numerical results depend upon the type of material.
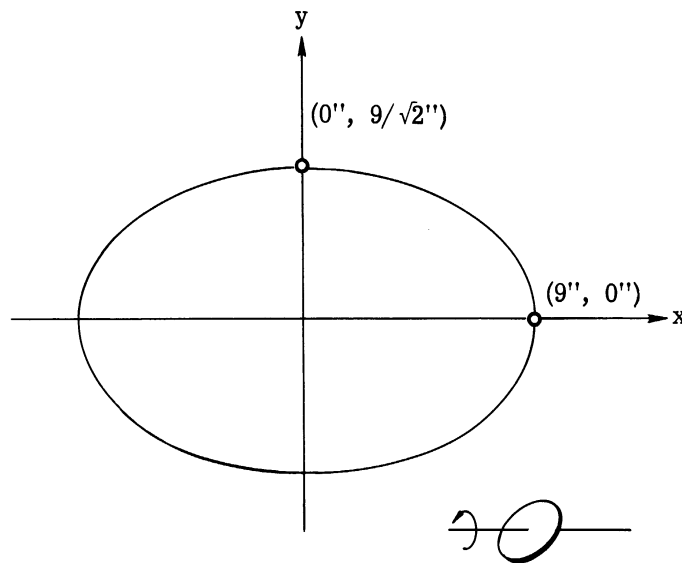
FIGURE 1. ROTATING ELLIPTICAL PLATE

The magnitudes of the stresses and deflections in a rotating plate depend in large measure on the method of supporting the plate. Two extremes may be considered: (1) the edge simply supported, or (2) the edge rigidly clamped. In the general case, something intermediate would be encountered. In no event would one consider a thin plate inclined to the axis of rotation rotating at high speed with no edge support, since the bending stresses would either shatter the plate or at least warp it hopelessly out of shape.

For a plate with a clamped edge, the results are:

(a) Maximum deflection: 0.223×10^{-3} inch

(b) Maximum bending stress: 406 psi along major axis
                                                    350 psi along minor axis

(c) Maximum shearing stress: 187 psi

(d) Maximum total tensile stress: 753.3 psi

For a simply supported plate, the maximum deflection is 1.1×10^{-3} inch. No stresses were calculated for this case.

In the general case, the deflection would fall somewhere between those given above, which are possibly 5 to 25 times the desirable limit for a high-resolution system. The deflection can be held to within a desirable tolerance by decreasing the area of the plate or by increasing its thickness, or both, as discussed in Section 6.2.

The maximum total tensile stress in the rotating elliptical plate under consideration is 753.3 psi, which is much less than the 7110-psi design limit of fused quartz. The practicality of using crown glass in such an application is marginal since the design limit of glass is generally assumed to be 1000 psi. However, the deflection curves are given for crown glass as well as for quartz in Figure 8.

2.1.2. ROTATING CIRCULAR PLATES. An analysis of a circular plate (Figure 2), of dimensions comparable to the elliptical plate described in Section 2.1.1, was made for the sake of comparing results. The plate is 0.5 inch thick and has a radius of 4.5 inches. The center of rotation is the center of the plate, and the axis of rotation is at an angle of inclination of 45° to the surface of the plate. The rotational speed is 5000 rpm. The plate is constructed of fused quartz, although, as in the elliptical case, only the numerical results depend upon the material.
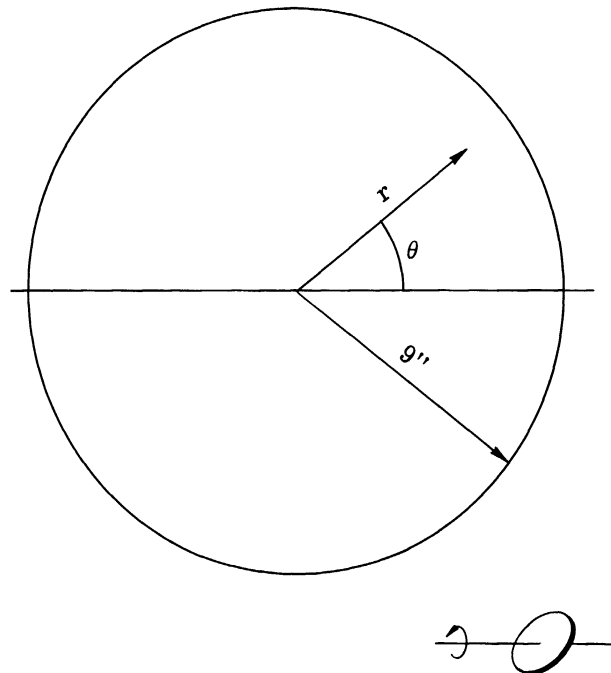
FIGURE 2. ROTATING CIRCULAR PLATE

If the plate has a clamped edge, the maximum deflection of the surface is 0.363×10^{-3} inch. This is the same magnitude as the deflection of the elliptical plate.

2.1.3. COMPARISON OF PLATE MATERIALS ON BASIS OF STRENGTH. A survey of the available materials for use in rotating plates showed that preference should be given as follows:

Clamped-Edge Case	Simply Supported Case
(1) $\begin{cases} \text{Aluminum} \\ \text{Fused Quartz} \end{cases}$	(1) $\begin{cases} \text{Quartz Fused} \\ \text{Molybdenum} \end{cases}$
(2) Molybdenum	(2) Aluminum
(3) Steel	(3) Steel
(4) Magnesium	(4) Magnesium
(5) Light Borate Crown	(5) Light Borate Crown

The difference between fused quartz and crown glass is not great enough to warrant giving serious consideration to the selection of a material on the basis of deflection alone, since in each case the crown glass deflects only 1.5 times as much as the fused quartz. The complete analysis of these materials is discussed in Section 6.1.

2.2. ROTATING TRIANGULAR PRISMS

A 6-inch-long fused-quartz prism, with a cross section in the form of an equilateral triangle 3 inches in altitude, is rotated at 100 rpm about the centroid of its cross section (Figure 10). The maximum deflection of the face of the prism, in a radial direction from the axis of rotation to the corners of the prism, is 12.6 μin.

The natural frequency of vibration of the prism is 8.17 kcs if the ends are simply supported and 18.8 kcs if the ends are clamped.

3
ROTATING ELLIPTICAL PLATES (CLAMPED EDGES)

A plate of elliptical shape is rotated about an axis passing through its center, the axis of rotation making a 45° angle with the major axis of the ellipse, as shown in Figure 3. The co-ordinate axes are such that the edge of the ellipse is described by the equation $(x/a)^2 + (y/b)^2 = 1$. The constants which describe the plate are

w = deflection of plate (inches)

ω = angular velocity of plate (radians/second)

q = load intensity (pounds/inch^2)

D = flexural rigidity of plate (inch-pounds)

E = Young's modulus (pounds/inch^2)

h = thickness of plate (inches)

ν = Poisson's ratio (inches/inch)

ρ = density of plate (pound-second^2/inch^4)
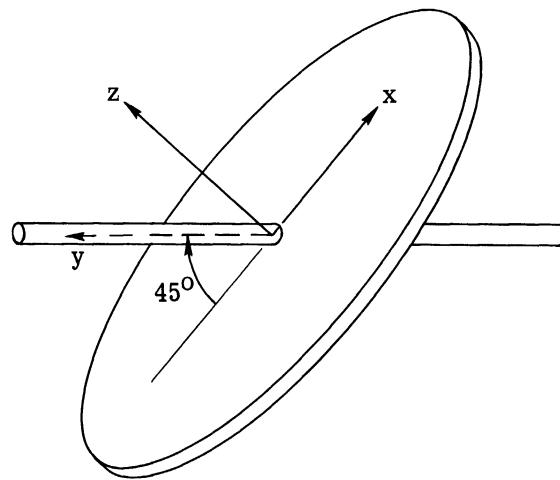
FIGURE 3. GEOMETRY OF ELLIPTICAL PLATE

3.1. DEFLECTIONS IN ELLIPTICAL PLATES

The equation governing the bending of plates (Reference 1) is $\nabla^4 w = q/D$. The load to which the plate is subjected is due entirely to the centrifugal forces in the plate (neglecting gravity), of which the normal component is distributed as shown in Figure 4. The load intensity on any element dA (Figure 4) is defined as the normal force per unit area. Hence,

$$q = \frac{\text{normal component of centrifugal force}}{dA} = \frac{\rho\omega^2 hx}{2}$$

The differential equation to be solved is therefore

$$\nabla^4 w = \frac{\rho\omega^2 hx}{2D}$$
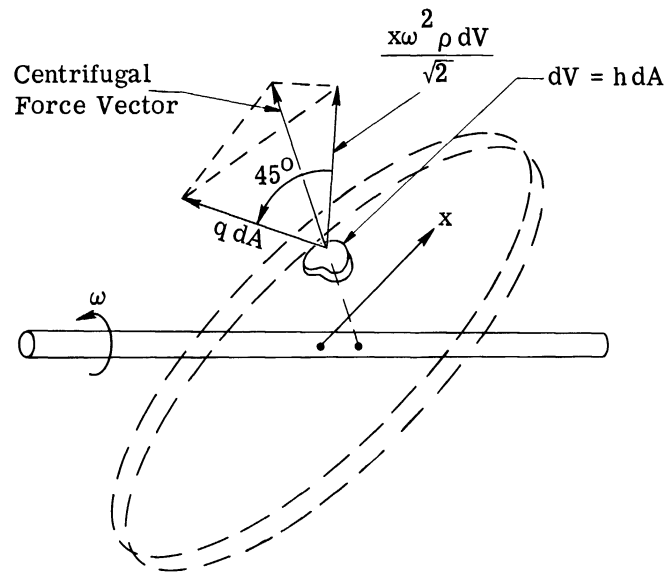
FIGURE 4. LOAD DISTRIBUTION ON ROTATING
ELLIPTICAL PLATE

Since the quantity D is the flexural rigidity and is given by the relationship

$$D = \frac{Eh^3}{12(1 - \nu^2)}$$

the final equation is

$$\nabla^4 w = \frac{12 \rho \omega^2 (1 - \nu^2) x}{2Eh^2}$$

The boundary conditions are:

$$\text{at } x = a, \qquad w = \frac{dw}{dx} = 0$$

A solution which satisfies the boundary conditions and also the differential equation is

$$w = \frac{\rho \omega^2 a^5 (1 - \nu^2)}{4Eh^2} \left[\frac{1}{5 + 2\left(\frac{a}{b}\right)^2 + \left(\frac{a}{b}\right)^4} \right] \left[1 - \left(\frac{x}{a}\right)^2 - \left(\frac{y}{a}\right)^2 \left(\frac{a}{b}\right)^2 \right] \left(\frac{x}{a}\right)$$

Since the major axis has the greatest dimension, the maximum deflection (W) will occur along the major axis. Differentiation of w with respect to x for $\cos \theta = 1$ and $\sin \theta = 0$ yields

$$x = \pm a, \ \pm \frac{a}{\sqrt{5}}$$

6

for $\frac{dw}{dx} = 0$. Since the deflection at $x = \pm a$ is zero, the maximum deflection must occur at $x = \pm \frac{a}{\sqrt{5}}$. Substituting this into the deflection equation,

$$W = \pm \frac{8}{25\sqrt{5}} \left[\frac{\rho \omega^2 a^5 (1 - \nu^2)}{26 E h^2} \right]$$

for $\frac{a}{b} = \sqrt{2}$.

Using the above relationships, the deflection may be calculated for any portion of the plate. The deflections along the major and minor axes for crown glass and fused-quartz elliptical plates are given in Figure 8.

3.2. BENDING STRESSES IN ELLIPTICAL PLATES

The bending stresses created in the plate may be calculated from the following relationships:

M_x = moment causing stresses in the x-direction

$$= -D \left(\frac{\partial^2 w}{\partial x^2} + \nu \frac{\partial^2 w}{\partial y^2} \right)$$

and σ_x = normal stress in the x-direction

$$= \frac{M_x (h/2)}{h^3/12}$$

or

$$\sigma_x = -\frac{6D}{h^2} \left(\frac{\partial^2 w}{\partial x^2} + \nu \frac{\partial^2 w}{\partial y^2} \right)$$

Combining the above with the solution for w obtained from the preceding calculation, the final result is

$$\sigma_x = \frac{\rho \omega^2 a^3}{8h} \left[\frac{1}{5 + 2\left(\frac{a}{b}\right)^2 + \left(\frac{a}{b}\right)^4} \right] \left\{ 8\left[\left(\frac{x}{a}\right)^3 + \nu\left(\frac{x}{a}\right)\left(\frac{y}{a}\right)^2\left(\frac{a}{b}\right)^4 \right] \right.$$
$$\left. - 4\left[1 - \left(\frac{x}{a}\right)^2 - \left(\frac{y}{a}\right)^2\left(\frac{a}{b}\right)^2 \right]\left[3\left(\frac{x}{a}\right) + \nu\left(\frac{x}{a}\right)\left(\frac{a}{b}\right)^2 \right] \right\}$$

Differentiation yields the result that the maximum stress occurs along the major axis at

$$x = \pm \frac{a}{\sqrt{5}} \left[\frac{1 + \frac{\nu}{3}\left(\frac{a}{b}\right)^2}{1 + \frac{\nu}{5}\left(\frac{a}{b}\right)^2} \right]^{1/2}$$

The value of the radical is very close to unity for reasonable values of Poisson's ratio ($\nu << 1$), so the maximum bending stress occurs near the point of maximum deflection $\left(\text{i. e. , at } x = \pm\frac{a}{5}\right)$. Hence, the maximum bending stress in the x-direction is

$$\left(\sigma_x\right)_{\text{maximum}} \cong \pm\frac{4}{13\sqrt{5}} \left(\frac{\rho\omega^2 a^3}{4h}\right)(1 + \nu)$$

Similarly, from the relationships

M_y = moment causing stresses in the y-direction

$$= -D\left[\frac{\partial^2 w}{\partial y^2} + \nu\frac{\partial^2 w}{\partial x^2} \right]$$

and

σ_y = normal stress in the y-direction

$$= \frac{M_y(h/2)}{(h^3/12)} = \frac{6M_y}{h^2}$$

or

$$\sigma_y = \frac{-6D}{h^2}\left(\frac{\partial^2 w}{\partial y^2} + \nu\frac{\partial^2 w}{\partial x^2}\right)$$

the normal stress in the y-direction is

$$\sigma_y = -\left(\frac{\rho\omega^2 a^3}{8h}\right)\left[\frac{1}{5 + 2\left(\frac{a}{b}\right)^2 + \left(\frac{a}{b}\right)^4} \right]\left\{ 8\left[\left(\frac{x}{a}\right)\left(\frac{y}{a}\right)^2\left(\frac{a}{b}\right)^4 \right.\right.$$
$$\left.\left. + \nu\left(\frac{x}{a}\right)^3\right] - 4\left[1 - \left(\frac{x}{a}\right)^2 - \left(\frac{y}{a}\right)^2\left(\frac{a}{b}\right)^2\right]\left[\left(\frac{x}{a}\right)\left(\frac{a}{b}\right)^2 + 3\nu\left(\frac{x}{a}\right)\right]\right\}$$

This function reaches its maximum at

$$y = 0$$

and

$$x = \pm \frac{a}{\sqrt{3}} \left[\frac{1 + 3\nu \left(\frac{b}{a}\right)^2}{1 + 5\nu \left(\frac{b}{a}\right)^2} \right]^{1/2}$$

which, for reasonable values of ν, is approximately $x = \pm \frac{a}{3}$. Hence

$$\left(\sigma_y\right)_{\text{maximum}} \cong \frac{8}{39\sqrt{3}} \left(\frac{\rho\omega^2 a^3}{4h}\right) (1 + \nu)$$

Since the ratio of the maximum stresses is

$$\frac{\left(\sigma_x\right)_{\text{maximum}}}{\left(\sigma_y\right)_{\text{maximum}}} = \sqrt{\frac{27}{20}}$$

the stresses are of the same order of magnitude.

3.3. SHEARING STRESSES IN ELLIPTICAL PLATES

The shearing stresses created in the plate are calculated from the following:

τ_{xy} = shearing stress of yz-plane in the y-direction

$$= -\left(\frac{E}{1 + \nu}\right) \left(\frac{h}{2}\right) \left(\frac{\partial^2 w}{\partial x \partial y}\right)$$

For the elliptical plate, the result is

$$\tau_{xy} = \left(\frac{\rho\omega^2 a^3}{8h}\right) (1 - \nu) \left[\frac{1}{5 + 2\left(\frac{a}{b}\right)^2 + \left(\frac{a}{b}\right)^4} \right] \left\{ 4\left(\frac{y}{a}\right)\left(\frac{a}{b}\right)^2 \left[1 \right. \right.$$

$$\left. - \left(\frac{x}{a}\right)^2 - \left(\frac{y}{a}\right)^2\left(\frac{a}{b}\right)^2 \right] - 8\left(\frac{x}{a}\right)^2\left(\frac{y}{a}\right)^2\left(\frac{a}{b}\right)^2 \right\}$$

It can be determined by differentiation that the maximum value of this function occurs along the y-axis at

$$y = \pm a \left[\frac{1}{3}\left(\frac{b}{a}\right)^2 \right]^{1/2}$$

The maximum shearing stress is therefore

$$\left(\tau_{xy}\right)_{\text{maximum}} = \pm \frac{8}{39\sqrt{6}} \left(\frac{\rho\omega^2 a^3}{4h}\right) (1 - \nu)$$

3.4. MAXIMUM TOTAL STRESS

The greatest total stress in the plate is of interest in that, if the plate cannot withstand the stress, regardless of how small the deflections, it obviously cannot suit the purpose for which it is intended.

The total bending stress at a point is given by the expression

$$\sigma_t = \sqrt{(\sigma_x)^2 + (\sigma_y)^2}$$

The centrifugal stress in a plate whose edges are restrained from expansion is given by

$$\sigma_r = -\frac{\rho\omega^2 a^2}{16}\left[2(3+\nu)\left(\frac{r}{a}\right)^2 - (1+\nu)\right]$$

The total stress will then be

$$(\sigma_r)^2 + (\sigma_t')^2 \le (\sigma_t)^2 \le \left(|\sigma_r| + |\sigma_t'|\right)^2$$

Taking the upper limit to allow an adequate margin of safety,

$$(\sigma_t)_{\text{maximum}} = \frac{\rho\omega^2 a^2}{13}\left[\left(\frac{a}{h}\right)(1+\nu^2)^{1/2} + \frac{13}{16}(5+\nu)\right]$$

this maximum occurring at (a, 0).

3.5. SAMPLE CALCULATIONS

Assume that the plate is made of fused quartz and has the following constants.

a = 4.5 inches

$b = \frac{a}{2}$

h = 0.5 inch

$E = 10.12 \times 10^6 \text{psi}$

$\nu = 0.144$ inch

$\omega = \frac{500\pi}{3}$ radians/second

$\rho = 2.07 \times 10^{-4}$ pound-second^2/inch^4

$$W = \pm\frac{B}{25\sqrt{5}}\left[\frac{\rho\omega^2 a^5(1-\nu^2)}{26Eh^2}\right] = \pm 0.233 \times 10^{-3} \text{ inch}$$

$$\left(\sigma_x\right)_{\text{maximum}} \cong \pm \frac{4}{13\sqrt{5}}\left(\frac{\rho\omega^2 a^3}{4h}\right)(1 + \nu) = \pm 406 \text{ psi}$$

$$\left(\sigma_y\right)_{\text{maximum}} \cong \pm \frac{8}{39\sqrt{3}}\left(\frac{\rho\omega^2 a^3}{4h}\right)(1 + \nu) = \pm 350 \text{ psi}$$

$$\left(\tau_{xy}\right)_{\text{maximum}} = \pm \frac{8}{39\sqrt{6}}\left(\frac{\rho\omega^2 a^2}{4h}\right)(1 - \nu) = \pm 187 \text{ psi}$$

$$\left(\sigma_t\right)_{\text{maximum}} = \frac{\rho\omega^2 a^2}{13}\left[\left(\frac{a}{h}\right)(1 + \nu^2)^{1/2} + \frac{13}{16}(5 + \nu)\right] = 753.3 \text{ psi}$$

4
ROTATING CIRCULAR PLATES (CLAMPED EDGES)

A plate of circular shape is rotated about an axis passing through its center, the axis of rotation being inclined at 45° to the surface of the plate, as shown in Figure 5. The plate edge is described by the equation $x^2 + y^2 = a^2$.
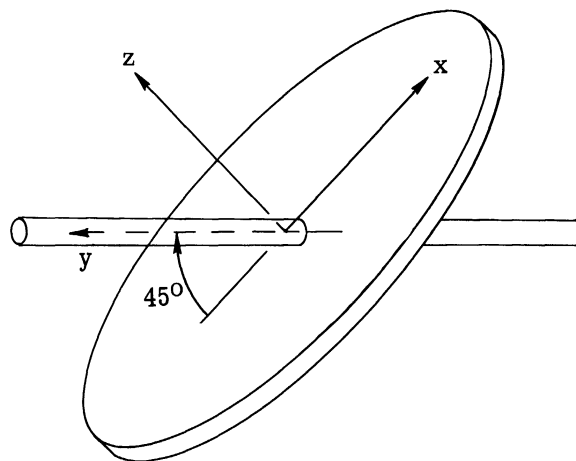

FIGURE 5.   GEOMETRY OF CIRCULAR PLATE

The constants which describe the plate are:

w = deflection of plate (inches)

ω = angular velocity of plate (radians/second)

q = load intensity (pounds/inch^2)

h = thickness of plate (inches)

D = flexural rigidity of plate (inch-pounds)

E = Young's modulus (pounds/inch^2)

ν = Poisson's ratio (inches/inch)

ρ = density of plate (pound-second^2/inch^4)

4.1. DEFLECTIONS IN CIRCULAR PLATES

The equation governing the bending of plates is $\nabla^4 w = q/D$. Using the concept of normal load intensity described in Section 3.1, the general solution (Reference 1) is

$$w = \frac{\rho\omega^2 a^5 (1 - \nu^2)}{32Eh^2} \left[\left(\frac{r}{a}\right)^5 + A\left(\frac{r}{a}\right) + B\left(\frac{r}{a}\right)^3 \right.$$

$$\left. + C\left(\frac{a}{r}\right) + D\left(\frac{r}{a}\right) \ell n\left(\frac{r}{a}\right) \right] \cos \theta$$

At the center of the plate, w and $\frac{\partial w}{\partial r}$ are both finite. Hence, C = D = 0. Also, along the edge of the plate,

$$w = \frac{\partial w}{\partial r} = 0$$

Using these boundary conditions, the final result becomes

$$w = \left[\frac{\rho\omega^2 a^5 (1 - \nu^2)}{32Eh^2} \right] \left[1 - \left(\frac{r}{a}\right)^2 \right] \left(\frac{r}{a}\right) \cos \theta$$

It should be noted that this is the same result as would be obtained by letting a = b, x = r cos θ, and y = r sin θ in the equation of the elliptical plate (Section 3.1). Hence, the validity of the equations is verified.

The maximum value of this function occurs at θ = 0 and r = $\pm\frac{a}{5}$. That is,

$$W = \pm \frac{8}{25\sqrt{5}} \left[\frac{\rho\omega^2 a^5 (1 - \nu^2)}{16Eh^2} \right]$$

4.2. SAMPLE CALCULATION

Assume that the plate is made of fused quartz and has the following constants:

   a = 4.5 inches

   h = 0.5 inch

   E = 10.12 x 10^6 psi

   ν = 0.144 inch/inch

   $\omega = \frac{500\pi}{3}$ radians/second

   ρ = 2.07 x 10^{-4} pound-second^2/inch^4

Then

$$W = \pm \frac{8}{25\sqrt{5}} \left[\frac{\rho\omega^2 a^5 (1 - \nu^2)}{16Eh^2} \right] = \pm 0.363 \times 10^{-3} \text{ inch}$$

5
ROTATING ELLIPTICAL PLATES (SIMPLY SUPPORTED EDGES)

Section 3 discussed the mechanics of rotating elliptical plates with clamped edges. However, in the general case, the edge of the plate is neither clamped nor simply supported, but rather is supported in some intermediate manner. Hence, the simply supported case should also be considered.

The required deflection curve must satisfy the relations

$$\nabla^4 w = q/D$$

and

$$w \text{ (boundary)} = 0$$

$$m \text{ (boundary)} = 0$$

After an unsuccessful attempt to find an exact solution to these equations, an approximation was used in order to determine the magnitude of deflection in a simply supported rotating elliptical plate.

The condition which is difficult to satisfy in the simply supported case is that which specifies that the moment be zero at the edge. A method of obtaining this is to find the deflection (Figure 6) caused by the edge moment in the clamped plate and subtract the result from the solution for the clamped-edge case. From Sections 3.1 and 3.2, the deflection and moment equations for the clamped-edge case are

$$w = \left[\frac{\rho\omega^2 a^5(1-\nu^2)}{4Eh^2}\right]\left[\frac{1}{5+2\left(\frac{a}{b}\right)^2+\left(\frac{a}{b}\right)^4}\right]\left[1-\left(\frac{x}{a}\right)^2\right.$$

$$\left.-\left(\frac{y}{a}\right)^2\left(\frac{a}{b}\right)^2\left(\frac{x}{a}\right)\right]$$

$$M_x = -\left(\frac{\rho\omega^2 ha^3}{48}\right)\left[\frac{1}{5+2\left(\frac{a}{b}\right)^2+\left(\frac{a}{b}\right)^4}\right]\left\{8\left[\left(\frac{x}{a}\right)^3\right.\right.$$

$$\left.+\nu\left(\frac{x}{a}\right)\left(\frac{y}{a}\right)^2\left(\frac{a}{b}\right)^4\right]-4\left[1-\left(\frac{x}{a}\right)^2-\left(\frac{y}{a}\right)^2\left(\frac{a}{b}\right)^2\right]\left[3\left(\frac{x}{a}\right)\right.$$

$$\left.\left.+\nu\left(\frac{x}{a}\right)\left(\frac{a}{b}\right)^2\right]\right\}$$

and

$$M_y = - \left(\frac{\rho\omega^2 h a^3}{48}\right)\left[-\frac{1}{5 + 2\left(\frac{a}{b}\right)^2 + \left(\frac{a}{b}\right)^4}\right]\left\{8\left[\left(\frac{x}{a}\right)\left(\frac{y}{a}\right)^2\left(\frac{a}{b}\right)^4\right.\right.$$

$$\left. + \nu\left(\frac{x}{a}\right)^3\right] - 4\left[1 - \left(\frac{x}{a}\right)^2 - \left(\frac{y}{a}\right)^2\left(\frac{a}{b}\right)^2\right]\left[\left(\frac{x}{a}\right)\left(\frac{a}{b}\right)^2 + 3\nu\left(\frac{x}{a}\right)\right]\right\}$$

FIGURE 6. PLATE ACTED UPON BY A BENDING
MOMENT ONLY

Since it was desired to find the deflection curves for lines passing through the point of maximum deflection, i.e., the point $\left(\frac{a}{\sqrt{5}},\ 0\right)$, the "equal and opposite" moments were applied at the points $\left(\frac{a}{\sqrt{5}},\ \frac{a\sqrt{2}}{\sqrt{5}}\right)$ and (a, 0) as shown in Figure 7. It should be noted that the results will be valid only for the lines y = 0 and x = $\frac{a}{\sqrt{5}}$.
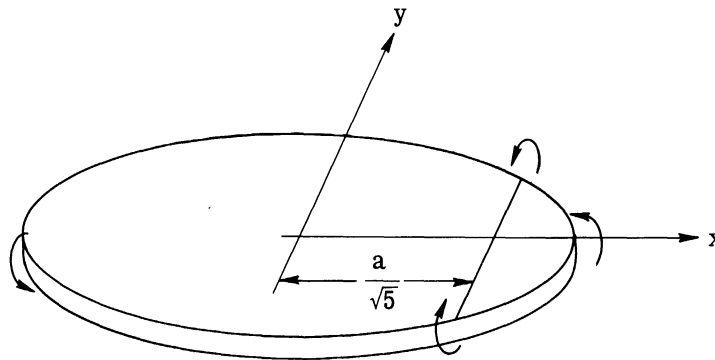

FIGURE 7. LOCATION OF MOMENTS APPLIED TO AN
ELLIPTICAL PLATE

The existing moment at (a, 0) in the clamped-edge plate is, for a = $\sqrt{2}$b,

$$M_1 = - \frac{\rho\omega^2 h a^3}{78}$$

At the point $\left(\dfrac{a}{\sqrt{5}}, \dfrac{a\sqrt{2}}{\sqrt{5}}\right)$, the moment is

$$M_2 = -\frac{\rho \omega^2 h a^3}{78}\left(\frac{8 + \nu}{5\sqrt{5}}\right)$$

where these moments act as shown in Figure 7.

Hence, the deflection of a plate acted upon only by the moments $M_x = -M_1$ and $M_y = -M_2$ may be computed, and the results superimposed upon the clamped-edge deflection curves to obtain the solution for the simply supported plate. From Section 3.2, the moments are related to the deflections by the expressions

$$M_x = -M_1 = -D\left(\frac{\partial^2 w}{\partial x^2} + \nu \frac{\partial^2 w}{\partial y^2}\right)$$

and

$$M_y = -M_2 = -D\left(\frac{\partial^2 w}{\partial y^2} + \nu \frac{\partial^2 w}{\partial x^2}\right)$$

These may be combined to give

$$\nabla^2 w = \frac{M_1 + M_2}{D(1 + \nu)}$$

for which the general solution is

$$w = \left[\frac{M_1 - \nu M_2}{2D(1 - \nu^2)}\right]x^2 + \left[\frac{M_2 - \nu M_1}{2D(1 - \nu^2)}\right]y^2 + a_1 x + b_1 y + c_1$$

The constants are evaluated from the following boundary conditions:

(1) At $(0, 0)$, $w = 0$

(2) At $(a, 0)$, $w = 0$

(3) At $\left(\dfrac{a}{\sqrt{5}}, \dfrac{a\sqrt{2}}{\sqrt{5}}\right)$, $w = 0$

From condition (1), $c_1 = 0$. From condition (2),

$$a_1 = -a\left[\frac{M_1 - \nu M_2}{2D(1 - \nu^2)}\right]$$

Finally, from condition (3)

$$b_1 = -\frac{a}{\sqrt{10}}\left\{\left[\frac{M_1 - \nu M_2}{2D(1 - \nu^2)}\right](1 - \sqrt{5}) + \left[\frac{M_2 - \nu M_1}{2D(1 - \nu^2)}\right]\right\} \quad (2)$$

For $a = \sqrt{2}b$, the solution for the deflection is therefore

$$w = \left(\frac{\rho\omega^2 a^5}{13Eh^2}\right)\left\{\left[1 + \left(\frac{8 + \nu}{5\sqrt{5}}\right)\nu\right]\left[\left(\frac{x}{a}\right)^2 - \left(\frac{x}{a}\right)\right] \right.$$

$$- \left(\frac{1 - \sqrt{5}}{\sqrt{10}}\right)\left(\frac{y}{a}\right)\right] + \left[\left(\frac{8 + \nu}{5\sqrt{5}}\right) - \nu\right]\left[\left(\frac{y}{a}\right)^2 \right.$$

$$\left. - \left(\frac{2}{\sqrt{10}}\right)\left(\frac{y}{a}\right)\right]\right\}$$

Once again, it should be noted that this equation applies only along the lines $y = 0$ and $x = \frac{a}{\sqrt{5}}$.

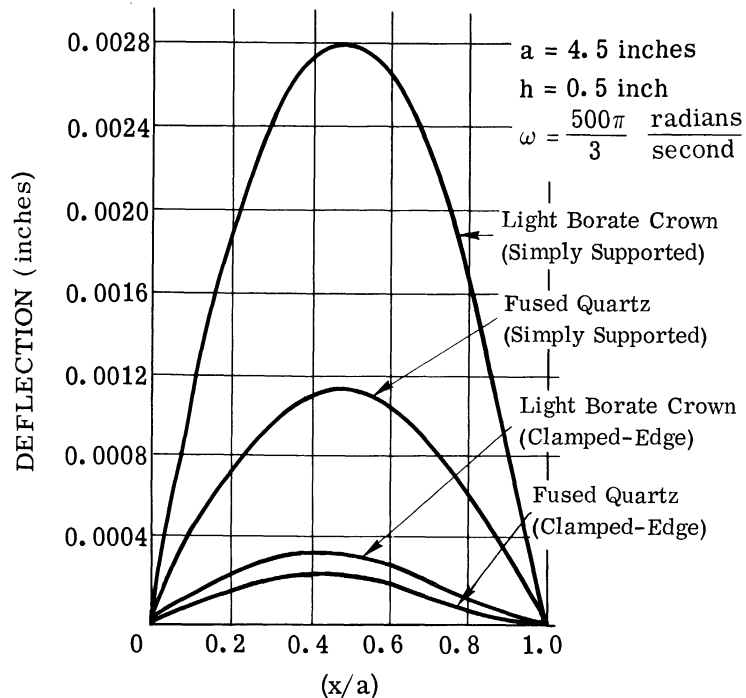The deflection curve for a simply supported elliptical plate (along $y = 0$) is given in Figure 8.

FIGURE 8.   DEFLECTIONS OF SIMPLY SUPPORTED AND
CLAMPED-EDGE ELLIPTICAL PLATES

6
COMPARISON of PLATE MATERIALS from VIEWPOINT of RIGIDITY

The deflection equation for a rotating elliptical plate, as discussed in Section 3, contains essentially two constants:

$$(1) \quad \begin{cases} \dfrac{\rho}{E}(1 - \nu^2) & \text{clamped edge} \\[2em] \dfrac{\rho}{E}\left[1 + \left(\dfrac{8 + \nu}{5\sqrt{5}}\right)\nu\right] & \text{simply supported edge} \end{cases}$$

$$(2) \quad \dfrac{\omega^2 a^5}{h^2}$$

The first of these depends only upon the material, whereas the second is a function of the plate geometry and rotational speed.

6.1. SURVEY OF MATERIALS

A comparison of the material-dependent constants for different plate materials can be easily made by using numbers from a reliable engineering handbook. The magnitude of the constants will be directly proportional to the magnitudes of the deflections for a fixed-speed and-geometry situation. Table I is a summary of the physical constants for seven plate materials.

TABLE I. PHYSICAL CONSTANTS FOR PLATE MATERIALS[*]

MATERIAL	$\rho \times 10^4$	ν	$E \times 10^{-6}$	$\dfrac{\rho}{E}(1 - \nu^2) \times 10^{10}$	$\dfrac{\rho}{E}\left[1 + \left(\dfrac{8 + \nu}{5\sqrt{5}}\right)\nu\right] \times 10^{10}$
Aluminum (98.3 Rolled)	2.55	0.47	10.10	0.197	0.425
Fused Quartz	2.07	0.14	10.12	0.201	0.355
Molybdenum	9.02	0.00	42.7	0.211	0.362
Steel (C.38 Annealed)	.7.35	0.24	29.01	0.239	0.440
Magnesium	1.64	0.25	6.06	0.254	0.471
Light Borate Crown	2.11	0.27	6.60	0.296	0.554
Celluloid	3.46	0.41	0.53	5.431	11.172

*See Reference 2.

It can be seen from Table I that (with the exception of celluloid) the selection of a plate material cannot be made on the basis of rigidity. However, other criteria (such as reflectivity, ultimate strength, and grain size) may be such as to confer preference upon a particular material for a given application.

6.2. RELATIONSHIP OF PLATE DIMENSIONS

Since the material constants do not offer much versatility for restricting plate deflections, the geometric constant $\frac{a^5}{h^2}$ (for constant speed) will be considered. It is clear that, for a given material and speed, the deflection is proportional to $\frac{a^5}{h^2}$. Hence, if a deflection w_0 is calculated for a particular $\frac{a_0^5}{h_0^2}$, the corresponding deflection w for any other $\frac{a^5}{h^5}$ may be obtained by inspection: $\left(\frac{w}{w_0}\right) = \left(\frac{a}{a_0}\right)^5\left(\frac{h_0}{h}\right)^2$. The relationship between a and h may be illustrated by a plot of $\left(\frac{a}{a_0}\right)$ versus $\left(\frac{h_0}{h}\right)$ for $\left(\frac{w}{w_0}\right)$ = constant, as shown in Figure 9. A decrease in deflection by approximately a factor of 10 is obtained by decreasing a to $\frac{2}{3}a_0$ or by increasing h to $3h_0$, whereas doing both at once gives a decrease in deflection by a factor of almost 100. The indication here is that a change in size is far more effective than a change in material as far as deflections are concerned.
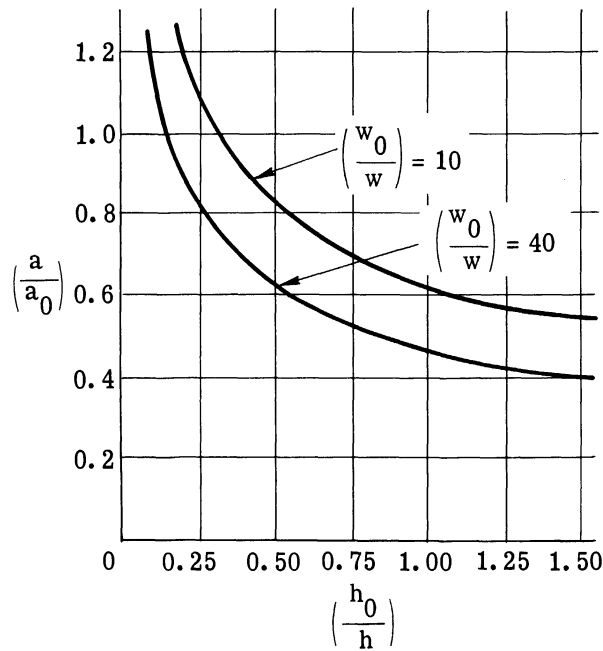

FIGURE 9. DIAMETER-THICKNESS RELATIONSHIPS
FOR ROTATING PLATES

<div align="center">

7

ROTATING TRIANGULAR PRISMS

</div>

The prism to be considered here has a cross section which is an equilateral triangle and a length which is greater than its greatest cross sectional dimension (Figure 10). The prism is acted upon by centrifugal forces resulting from rotation about an axis passing through its centroid.

7. 1. DEFLECTIONS IN ROTATING TRIANGULAR PRISMS

Using the same notations for stress as before, the equations of equilibrium for the prism are

$$\frac{\partial \sigma_r}{\partial r} + \frac{1}{r}\frac{\partial \tau_{r\theta}}{\partial \theta} + \frac{\sigma_r - \sigma_\theta}{r} + R = 0$$

and

$$\frac{1}{r}\frac{\partial \sigma_\theta}{\partial \theta} + \frac{\partial \tau_{r\theta}}{\partial r} + \frac{2\tau_{r\theta}}{r} = 0$$

where R is the body force (per unit volume) in the prism. The body force may be expressed in terms of a potential function V:

$$R = -\frac{\partial V}{\partial r}$$

$$V = -\frac{1}{2}\rho\omega^2 r^2$$

A system of stresses which satisfies equilibrium is

$$\sigma_r = \frac{1}{r}\frac{\partial \phi}{\partial r} + \frac{1}{r^2}\frac{\partial^2 \phi}{\partial \theta^2} + V$$

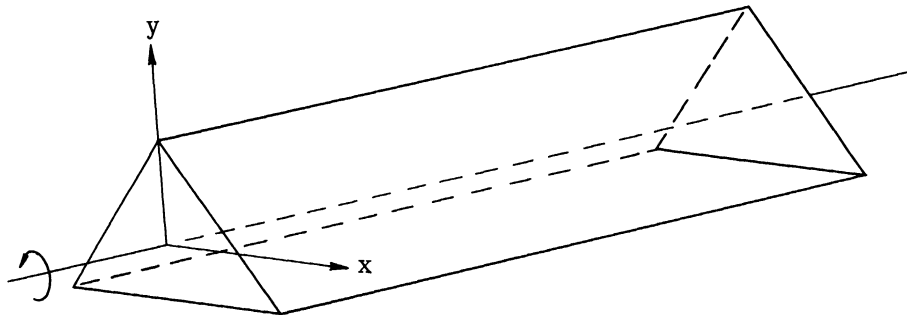$$\sigma_\theta = \frac{\partial^2 \phi}{\partial r^2} + V$$

FIGURE 10. GEOMETRY OF ROTATING PRISM

and

$$\tau_{r\theta} = -\frac{\partial}{\partial r}\left(\frac{1}{r}\frac{\partial\phi}{\partial\theta}\right)$$

where ϕ is a stress function.

The general two-dimensional stress function in polar coordinates (Reference 2) is

$$\phi = A \ln r + Br^2 + Cr^2 \ln r + Dr^2\theta + E\theta$$

$$+ \frac{a_1}{2}r\theta \sin \theta + \left(b_1 r^3 + a_1' r^{-1} + b_1' r \ln r\right) \cos \theta$$

$$+ \frac{c_1}{2}r\theta \cos \theta + \left(d_1 r^3 + c_1' r^{-1} + d_1' r \ln r\right) \sin \theta$$

$$+ \sum_{n=2}^{\infty} \left(a_n r^n + b_n r^{n+2} + a_n' r^{-n} + b_n' r^{2-n}\right) \cos n\theta$$

$$+ \sum_{n=2}^{\infty} \left(c_n r^n + d_n r^{n+2} + c_n' r^{-n} + d_n' r^{2-n}\right) \sin n\theta + \phi_1$$

where ϕ_1 is the particular solution of the compatability equation

$$\nabla^4\phi = -\left(\frac{1 - 2\nu}{1 - \nu}\right)\nabla^2 V = 2\left(\frac{1 - 2\nu}{1 - \nu}\right)\rho\omega^2$$

This is the governing equation for the case of plane strain (no axial deformation). For plane stress (no axial stress) the compatability equation is

$$\nabla^4\phi = -(1 - \nu)\nabla^2 V = 2(1 - \nu)\rho\omega^2$$

which, for $\nu << 1$, is the same as for plane strain.

The displacements in the prism are (for plane strain)

$$u_r = \frac{1 + \nu}{E}\int\left[(1 - \nu)\sigma_r - \nu\sigma_\theta\right] dr + f(\theta)$$

and

$$u_\theta = \frac{1 + \nu}{E}\int\left[(1 - \nu)\sigma_\theta - \nu\sigma_r\right] d\theta - \int u_r d\theta + g(r)$$

From the symmetry of the prism,

$$u_r(\theta) = u_r(-\theta) = u_r\left(\theta + \frac{2\pi}{3}\right)$$

and

$$u_\theta(\theta) = -u_\theta(-\theta) = u_\theta\left(\theta + \frac{2\pi}{3}\right)$$

The stress-displacement relationships may be derived as follows:

$$\sigma_r = \Sigma a_n \sin n\theta + \Sigma b_n \cos n\theta + \Sigma c_n$$

and

$$\sigma_\theta = \Sigma d_n \sin n\theta + \Sigma e_n \cos n\theta + \Sigma f_n$$

where a, b, c, d, e, and f are not functions of θ. Hence

$$u_r = \frac{1+\nu}{E}\left\{\Sigma \sin n\theta \int \left[(1-\nu)a_n - \nu d_n\right]dr\right.$$

$$+ \Sigma \cos n\theta \int \left[(1-\nu)b_n - \nu e_n\right]dr + \Sigma \int \left[(1-\nu)c_n - \nu f_n\right]dr$$

$$\left. + \frac{Ef(\theta)}{1+\nu}\right\}$$

and

$$u_\theta = \frac{1+\nu}{E}\left(\Sigma \frac{\cos n\theta}{n}\left\{\left[\nu a_n - (1-\nu)d_n\right]r\right.\right.$$

$$+ \int \left[(1-\nu)a_n - \nu d_n\right]dr\right\} + \Sigma \frac{\sin n\theta}{n}\left\{\left[(1-\nu)e_n - \nu b_n\right]r\right.$$

$$+ \int \left[(1-\nu)b_n - \nu e_n\right]dr\right\} + r\theta \Sigma c_n + \theta \Sigma \int \left[(1-\nu)c_n - \nu f_n\right]dr$$

$$\left. + \frac{Eg(r)}{1+\nu}\right)$$

Since $u_\theta(\theta) = -u_\theta(-\theta)$ and $u_r(\theta) = u_r(-\theta)$, c_n and f_n must be independent, or r and $a_n = d_n = g(r) = 0$. Also, since the displacement at the center is zero,

$$f(\theta) = 0$$

Any terms which yield infinite stresses at the center must also be zero, so the final stress function is

$$\phi = Br^2 + \sum_{n=1}^{\infty} \left(a_n r^{3n} + b_n r^{3n+2}\right) \cos 3n\theta + \phi_1$$

Since the forces are only functions of r, let

$$\phi_1 = \left(\frac{1 - \nu}{12}\right)\rho\omega^2 r^4$$

Letting

$$\left(\frac{1 - 2\nu}{1 - \nu}\right) = (1 - \nu)$$

the associated stresses become

$$\sigma_r = 2B - \sum_{n=1}^{\infty} \left\{\left[3n(3n - 1)a_n r^{3n-2}\right] + \left[(3n - 2)(3n - 1)b_n r^{3n}\right]\right\} \cos 3n\theta$$

$$- \left(\frac{3 + \nu}{8}\right)\rho\omega^2 r^2$$

and

$$\sigma_\theta = 2B + \sum_{n=1}^{\infty} \left\{\left[3n(3n - 1)a_n r^{3n-2}\right] + \left[(3n + 2)(3n - 1)b_n r^{3n}\right]\right\} \cos 3n\theta$$

$$- \left(\frac{1 + 3\nu}{8}\right)\rho\omega^2 r^2$$

An approximate solution is obtained by using n = 1 and n = 2 in the above equations.

Along the face of the prism,

$$r = \frac{2b}{\sqrt{3}\,\sin\theta + \cos\theta}$$

and the normal stress is

$$\sigma_n = \sigma_r \cos\left(\frac{\pi}{3} - \theta\right) + \sigma_\theta \sin\left(\frac{\pi}{3} - \theta\right) = 0$$

These conditions are applied at the four points indicated in Figure 11, yielding the following results:

$$
\sigma_r = \rho\omega^2 b^2 \left\{ (0.424 + 0.286\nu) + \left[(0.151 + 0.214\nu)\left(\frac{r}{b}\right) \right. \right.
$$

$$
\left. - (0.019 + 0.054\nu)\left(\frac{r}{b}\right)^3 \right] \cos 3\theta + \left[(0.092 - 0.005\nu)\left(\frac{r}{b}\right)^4 \right.
$$

$$
\left. \left. - (0.009 - 0.005\nu)\left(\frac{r}{b}\right)^6 \right] \cos 6\theta - (0.375 + 0.125\nu) \right\}
$$

and

$$
\sigma_\theta = \rho\omega^2 b^2 \left\{ (0.424 + 0.286\nu) \right.
$$

$$
- \left[(0.151 + 0.214\nu)\left(\frac{r}{b}\right) - (0.096 + 0.268\nu)\left(\frac{r}{b}\right)^3 \right] \cos 3\theta
$$

$$
- \left[(0.092 - 0.005\nu)\left(\frac{r}{b}\right)^4 - (0.017 - 0.009\nu)\left(\frac{r}{b}\right)^6 \right] \cos 6\theta
$$

$$
\left. - (0.125 + 0.375\nu) \right\}
$$

It may be shown by differentiation that the maximum stress will be the radial stress at $\theta = 0$, $\left(\frac{r}{b}\right) = \dfrac{0.60 + 0.86\nu}{3 + \nu}$. For small values of ν this is
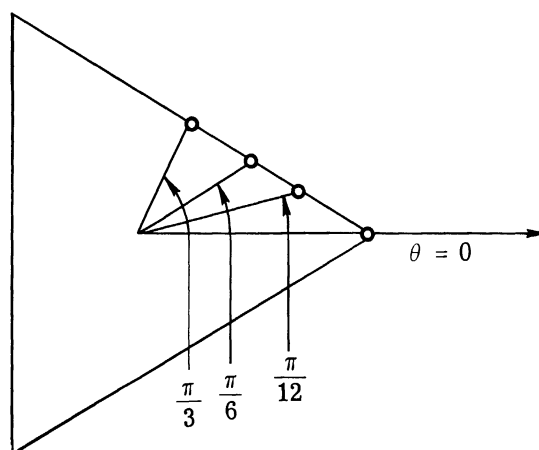
$$
\frac{r}{b} \cong 0.201 + 0.352\nu
$$

FIGURE 11. POINTS USED IN SOLUTION OF PRISM
EQUATIONS

The maximum radial stress is therefore

$$\left(\sigma_r\right)_{maximum} \cong \frac{1}{12}\rho\omega^2 b^2 (1 + 3\nu)$$

The radial displacement is given by the relationship

$$u_r = \frac{\rho\omega^2 b^3 (1 + \nu)}{32E}\left\{(13.56 + 9.14\nu)(1 - 2\nu)\left(\frac{r}{b}\right)\right.$$

$$+ \left[(2.417 + 3.424\nu)\left(\frac{r}{b}\right)^2 - (0.153 + 0.429\nu)\left(\frac{r}{b}\right)^4\right]\cos 3\theta$$

$$+ \left.\left[(0.588 - 0.029\nu)(1 - 4\nu)\left(\frac{r}{b}\right)^5 - (0.039 - 0.020\nu)(1 + \nu)\left(\frac{r}{b}\right)^7\right]\cos 6\theta\right\}$$

The above relationships are valid for $\theta = 0$, $\frac{\pi}{12}$, $\frac{\pi}{6}$, and $\frac{\pi}{3}$. The maximum radial displacement is

$$\left(u_r\right)_{maximum} = \frac{\rho\omega^2 b^2 (1 + \nu)}{32E}(48 - 36\nu + 38\nu^2)$$

at $r = 2b$ and $\theta = 0$.

7.2 VIBRATIONS IN ROTATING PRISMS

Section 7.1 discussed the stresses and deflections in a rotating triangular prism whose length is much greater than its greatest cross-sectional dimension. The sample calculations (Section 7.3) indicate that the stresses and deflections caused by centrifugal forces in the member are very small in magnitude, even for applications involving large prisms rotating at high speeds. Another effect encountered in rotating members of this type is vibration caused by dynamic unbalance in the prism itself. Such an effect may be encountered in any rotating shaft whose length is greater than its cross-sectional dimensions.

Reference 1 gives the expressions for the natural frequencies of clamped-end and simply supported beams in free vibration, involving a procedure developed by Lord Rayleigh. Using the constants

L = length of prism

I = moment of inertia of the prism cross section = $\displaystyle\iint_A y^2\, dA$

E = Young's modulus of elasticity

m = mass of prism

ω = angular velocity of prism

24

the corresponding natural frequencies are

$$f_{c_1} = \frac{\pi}{2} \sqrt{\frac{EI}{mL^2}}$$

for the simply supported member, and

$$f_{c_2} = \frac{2\pi}{\sqrt{3}} \sqrt{\frac{EI}{mL^2}}$$

for the clamped-end member. If the prism rotates at its natural frequency, any unbalance will cause resonance leading to an infinite amplitude of vibration. Due to the large magnitude of E, the natural frequencies are of the order of kilocycles. Since the amplitude of the vibration is always proportional to $\dfrac{1}{1 - (f/fc)^2}$, then for $f < < < f_c$ the amplitude will be very small.

7.3. SAMPLE CALCULATIONS

The triangular prism shown in Figure 12 is rotated about the centroid of its cross section, which is an equilateral triangle $2\sqrt{3}$ inches on a side. The prism is 6 inches long, and is made of fused quartz with a density of 2.07×10^{-4} (pound-second^2/inch^4) and Young's modulus of 10.12×10^6 psi.

$$(\sigma_r)_{maximum} = \frac{1}{12}\rho\omega^2 b^2 (1 + 3\nu) = 9.44 \text{ psi}$$

$$(u_r)_{maximum} = \frac{\rho\omega^2 b^3 (1 + \nu)}{32E} (48 - 36\nu + 38\nu^2) = 12.6 \times 10^{-6} \text{ inch}$$

The mass of the prism is

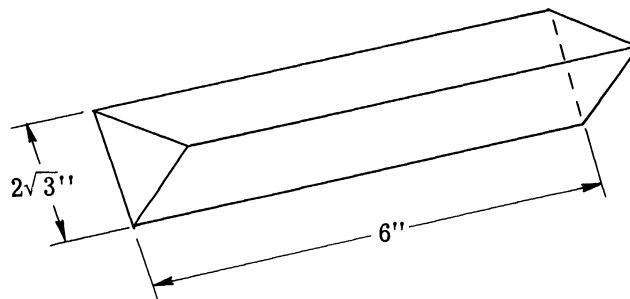$$m = \rho \left[\frac{1}{2}(2\sqrt{3}b)(3b)L \right] = 64.5 \times 10^{-4} \text{ (pound-second}^2\text{/inch)}$$

FIGURE 12. ROTATING TRIANGULAR PRISM

The moment of inertia of the cross section is

$$I = \iint_A y^2 \, dA = 3.75 \text{ (inches}^4\text{)}$$

The natural frequencies are therefore

$$f_{c_1} = \frac{\pi}{2} \sqrt{\frac{EI}{mL^3}} = 8.17 \text{ kcs}$$

and

$$f_{c_2} = \frac{2\pi}{\sqrt{3}} \sqrt{\frac{EI}{mL^3}} = 18.8 \text{ kcs}$$

REFERENCES

1. S. Timoshenko, Theory of Plates and Shells, 2nd ed., McGraw-Hill, New York, N. Y., 1959.

2. S. Timoshenko, Theory of Elasticity, McGraw-Hill, New York, N. Y., 1934

3. J. P. Den Hartog, Mechanical Vibrations, McGraw-Hill, New York, N. Y., 1934.

PROJECT MICHIGAN DISTRIBUTION LIST 7
1 February 1961 — Effective Date

Copy No.	Addressee
1	Army Research Office, ORCD, DA Washington 25, D. C. ATTN: Research Support Division
2-3	Commanding General U. S. Army Combat Surveillance Agency 1124 N. Highland Street Arlington 1, Virginia
4-40	Commanding Officer U. S. Army Signal Research & Development Laboratory Fort Monmouth, New Jersey ATTN: SIGRA/SL-ADT
41-42	Commanding General U. S. Army Electronic Proving Ground Fort Huachuca, Arizona ATTN: Technical Library
43	Chief, Human Factors Research Division Office of the Chief of Research & Development Department of the Army, Washington 25, D. C.
44-45	Commander, Army Rocket & Guided Missile Agency Redstone Arsenal, Alabama ATTN: Technical Library, ORDXR-OTL
46-47	Commanding Officer U. S. Army Transportation Research Command Fort Eustis, Virginia ATTN: Research Reference Center
48	Commanding General Army Medical Research & Development Command Main Navy Building, Washington 25, D. C. ATTN: Neuropsychiatry & Psychophysiology Research Branch
49	Commanding Officer, Ordnance Weapons Command Rock Island, Illinois ATTN: ORDOW-GN
50-53	Director, U. S. Army Engineer Research & Development Laboratories Fort Belvoir, Virginia
(50)	ATTN: Chief, Topographic Engineer Department
(51-52)	ATTN: Chief, Electrical Engineering Department
(53)	ATTN: Technical Documents Center
54	Commandant, U. S. Army War College Carlisle Barracks, Pennsylvania ATTN: Library
55	Commandant, U. S. Army Command & General Staff College Fort Leavenworth, Kansas ATTN: Archives

Copy No.	Addressee
56	Commandant, U. S. Army Infantry School Fort Benning, Georgia ATTN: Combat Developments Office
57-58	Assistant Commandant U. S. Army Artillery & Missile School Fort Sill, Oklahoma
59	Assistant Commandant, U. S. Army Air Defense School Fort Bliss, Texas
60	Commandant, U. S. Army Engineer School Fort Belvoir, Virginia ATTN: ESSY-L
61	Commandant, U. S. Army Signal School Fort Monmouth, New Jersey ATTN: SIGFM/SC-DO
62	Commandant, U. S. Army Aviation School Fort Rucker, Alabama ATTN: CDO
63-64	President, U. S. Army Intelligence Board Fort Holabird, Baltimore 19, Maryland
65	Commanding Officer, U. S. Army Signal Electronic Research Unit, P. O. Box 205 Mountain View, California
66-69	Office of Naval Research, Department of the Navy 17th & Constitution Avenue, N. W. Washington 25, D. C.
(66-67)	ATTN: Code 463
(68-69)	ATTN: Code 461
70	The Hydrographer, U. S. Navy Hydrographic Office Washington 25, D. C. ATTN: Code 4100
71	Chief, Bureau of Ships Department of the Navy, Washington 25, D. C. ATTN: Code 690
72-73	Director, U. S. Naval Research Laboratory Washington 25, D. C. ATTN: Code 2027
74	Commanding Officer, U. S. Navy Ordnance Laboratory Corona, California ATTN: Library
75	Commanding Officer & Director U. S. Navy Electronics Laboratory San Diego 52, California ATTN: Library
76-77	Department of the Air Force, Headquarters, USAF Washington 25, D. C. ATTN: AFOIN-1B1
78	Commander in Chief, Headquarters Strategic Air Command, Offutt Air Force Base, Nebraska ATTN: DINC

Distribution List 7, 1 February 1961 — Effective Date

Copy No.	Addressee
79	Aerospace Technical Intelligence Center U. S. Air Force Wright-Patterson AFB, Ohio ATTN: AFCIN-4B1a, Library
80-89	ASTIA (TIPCR) Arlington Hall Station, Arlington 12, Virginia
90-98	Commander, Wright Air Development Division Wright-Patterson AFB, Ohio
(90-93) (94) (95) (96-98)	ATTN: WWDE ATTN: WWAD-DIST ATTN: WWRDLP-2 ATTN: WWRNOO (Staff Physicist)
99-100	Commander, Rome Air Development Center Griffiss AFB, New York
(99) (100)	ATTN: RCOIL-2 ATTN: RCWIP-3
101-103	Commander, AF Command & Control Development Division Laurence G. Hanscom Field Bedford, Massachusetts ATTN: CCRHA-Stop 36
104	APGC(PGTRI) Eglin Air Force Base, Florida
105-108	Central Intelligence Agency 2430 E Street, N. W. Washington 25, D. C. ATTN: OCR Mail Room
109-114	National Aeronautics & Space Administration 1520 H Street, N. W. Washington 25, D. C.
115	Combat Surveillance Project Cornell Aeronautical Laboratory, Inc. Box 168, Arlington 10, Virginia ATTN: Technical Library
116	The RAND Corporation 1700 Main Street Santa Monica, California ATTN: Library
117-118	Cornell Aeronautical Laboratory, Inc. 4455 Genesee Street Buffalo 21, New York ATTN: Librarian VIA: Bureau of Naval Weapons Representative 4455 Genesee Street Buffalo 21, New York
119-120	Director, Human Resources Research Office The George Washington University P. O. Box 3596, Washington 7, D. C. ATTN: Library
121	Chief, U. S. Army Air Defense Human Research Unit Fort Bliss, Texas ATTN: Library

Copy No.	Addressee
122	Chief, U. S. Army Armor Human Research Unit Fort Knox, Kentucky ATTN: Security Officer
123	Chief, U. S. Army Infantry Human Research Unit P. O. Box 2086 Fort Benning, Georgia
124	Chief, USA Leadership Human Research Unit P. O. Box 2086, Presidio of Monterey, California
125	Chief Scientist, Department of the Army Office of the Chief Signal Officer Research & Development Division, SIGRD-2 Washington 25, D. C.
126	Columbia University Electronics Research Laboratories 632 W. 125th Street New York 27, New York ATTN: Technical Library VIA: Commander, Rome Air Development Center Griffiss AFB, New York ATTN: RCKCS
127	Coordinated Science Laboratory University of Illinois, Urbana Illinois ATTN: Librarian VIA: ONR Resident Representative 605 S. Goodwin Avenue Urbana, Illinois
128	Polytechnic Institute of Brooklyn 55 Johnson Street Brooklyn 1, New York ATTN: Microwave Research Institute Library VIA: Air Force Office of Scientific Research Washington 25, D. C.
129	Visibility Laboratory Scripps Institution of Oceanography University of California, San Diego 52, California VIA: ONR Resident Representative, University of California Scripps Institution of Oceanography, Bldg. 349 La Jolla, California
130	U. S. Army Aviation, Human Research Unit U. S. Continental Army Command P. O. Box 428, Fort Rucker, Alabama
131	Commanding General Quartermaster Research & Engineering Command U. S. Army, Natick, Massachusetts
132	Cooley Electronics Laboratory University of Michigan Research Institute Ann Arbor, Michigan ATTN: Director
133	U. S. Continental Army Command Liaison Officer, Project MICHIGAN The University of Michigan P. O. Box 618, Ann Arbor, Michigan
134	Commanding Officer, U. S. Army Liaison Group, Project MICHIGAN The University of Michigan P. O. Box 618, Ann Arbor, Michigan

AD   Div. 6/3

Institute of Science and Technology, U. of Michigan, Ann Arbor
MECHANICS OF ROTATING PLATES AND PRISMS by W. L. Brown
and C. T. Yang. Rept. of Proj. MICHIGAN. Feb 61. 26 p. incl.
illus., table, 3 refs.
(Rept. no. 2900-251-T)   Unclassified report
(Contract DA-36-039 SC-78801)

This is the report of an analysis of rotating plates and prisms from
a theoretical viewpoint for the purpose of setting limits on the size
and rotational speed of such bodies for scanner applications. The
analysis was carried completely through for a fused-quartz ellipti-
cal plate rotating about an axis, in the plane which contains a normal
to the plate and the major axis, at a 45° angle to the major axis, and
for a fused-quartz prism of triangular cross section rotating about
an axis through its centroid, normal to the cross section. The anal-
ysis indicated that the stresses and displacements are quite large
for a 0.5-inch-thick plate with a 9-inch major axis and a 9/2-inch
minor axis, but negligible for a 6-inch prism whose cross section is
                                                                  (over)

I.   Title: Project MICHIGAN
II. Brown, W. L., Yang, C. T.
III. U. S. Army Signal Corps
IV. Contract DA-36-039 SC-78801

Armed Services
Technical Information Agency

UNCLASSIFIED

DESCRIPTORS

Infrared scanner
Prisms
Mechanics
Rotation

AD

an equilateral triangle of 3-inch altitude. The foregoing applies for rotational frequencies of approximately 100 cps, which is a typical operating speed for an infrared scanner.

UNCLASSIFIED

UNCLASSIFIED

DESCRIPTORS

Infrared scanner
Prisms
Mechanics
Rotation

AD

an equilateral triangle of 3-inch altitude. The foregoing applies for rotational frequencies of approximately 100 cps, which is a typical operating speed for an infrared scanner.

UNCLASSIFIED

UNCLASSIFIED

DESCRIPTORS

Infrared scanner
Prisms
Mechanics
Rotation

AD

an equilateral triangle of 3-inch altitude. The foregoing applies for rotational frequencies of approximately 100 cps, which is a typical operating speed for an infrared scanner.

UNCLASSIFIED

UNCLASSIFIED

DESCRIPTORS

Infrared scanner
Prisms
Mechanics
Rotation

AD

an equilateral triangle of 3-inch altitude. The foregoing applies for rotational frequencies of approximately 100 cps, which is a typical operating speed for an infrared scanner.

UNCLASSIFIED

AD

Div. 6/3

Institute of Science and Technology, U. of Michigan, Ann Arbor
DYNAMIC BALANCING OF SCANNER DRUM AND GYROSCOPIC
EFFECT DURING MANEUVERS OF AIRCRAFT by W. L. Brown
and C. T. Yang. Rept. of Proj. MICHIGAN. Feb 61. 12 p. incl.
illus.
(Rept. no. 2900-250-T)   Unclassified report
(Contract DA-36-039 SC-78801)

This report presents the equations for determining the dynamic
balancing and gyroscopic effect of a rotating scanner drum assem-
bly of the type used in the Project MICHIGAN wide-angle scanner.
The parameters used in the numerical example are those of the
wide-angle scanner, and the theoretical calculations of the dynamic
balancing agree excellently with the actual mechanical dynamic bal-
ancing of the drum assembly. The calculations also indicate that
gyroscopic forces in the drum are negligible even during maximum
rate of turn and maximum rate of climb of the aircraft carrying the
scanner.
                                        (over)

UNCLASSIFIED

I.   Title: Project MICHIGAN
II. Brown, W. L., Yang, C. T.
III. U. S. Army Signal Corps
IV. Contract DA-36-039
     SC-78801

Armed Services
Technical Information Agency
UNCLASSIFIED

AD

UNCLASSIFIED

DESCRIPTORS

Infrared detection
Infrared scanners
Mathematical analysis
Equations

UNCLASSIFIED

AD

UNCLASSIFIED

DESCRIPTORS

Infrared detection
Infrared scanners
Mathematical analysis
Equations

UNCLASSIFIED

AD

UNCLASSIFIED

DESCRIPTORS

Infrared detection
Infrared scanners
Mathematical analysis
Equations

UNCLASSIFIED

AD

UNCLASSIFIED

DESCRIPTORS

Infrared detection
Infrared scanners
Mathematical analysis
Equations

UNCLASSIFIED